

APPENDIX

A. Proof of Theorem 1

Theorem 1: The proposed unified Benders cuts are valid because they do not eliminate the optimal solution for the original problem (4a)-(4d).

Proof: The original problem (4a)-(4d) is equivalent to:

$$\begin{aligned} & \min_{\mathbf{x}'} \mathbf{a}'^T \mathbf{x}' \\ & \text{s.t. } \mathbf{A}' \mathbf{x}' \geq \mathbf{d}' \\ & \quad \mathbf{B}'_i \mathbf{x}' + \mathbf{C}'_i \mathbf{y}_i + \mathbf{D}'_i \mathbf{z}_i \geq \mathbf{e}'_i, \quad \forall i \\ & \quad \mathbf{z}_i \in \{0,1\}^{K_i}, \quad \forall i \end{aligned}$$

which also achieves the same optimal solution as that of (4a)-(4d).

Let $\bar{\mathbf{x}}'$ be the optimal solution for \mathbf{x}' . For each unified dual subproblem parameterized by $\bar{\mathbf{x}}'$, the optimal solution $(\hat{\boldsymbol{\mu}}_i, \hat{\boldsymbol{\omega}}_i)$ must satisfy the following inequality:

$$(\mathbf{e}'_i - \mathbf{B}'_i \bar{\mathbf{x}}')^T \hat{\boldsymbol{\mu}}_i + \mathbf{1}^T \hat{\boldsymbol{\omega}}_i \leq 0, \quad \forall i$$

where $(\hat{\boldsymbol{\mu}}_i, \hat{\boldsymbol{\omega}}_i) = \arg \max_{(\boldsymbol{\mu}_i, \boldsymbol{\omega}_i) \in \mathcal{Q}_i, \boldsymbol{\omega}_i \in \mathcal{O}_i} \{(\mathbf{e}'_i - \mathbf{B}'_i \bar{\mathbf{x}}')^T \boldsymbol{\mu}_i + \mathbf{1}^T \boldsymbol{\omega}_i\}$.

Otherwise, the objective function of the primal unified subproblem achieves a positive optimal value. Hence, either the requested power exchanges violate limitations in the microgrid operation or the microgrid operation cost approximated by DSO is not accurate, which violates the optimality of $\bar{\mathbf{x}}'$.

Let $(\hat{\boldsymbol{\mu}}_i, \hat{\boldsymbol{\omega}}_i)$ be any set of coefficients in the unified Benders cuts generated at previous iterations such that $(\hat{\boldsymbol{\mu}}_i, \hat{\boldsymbol{\omega}}_i)$ is an optimal solution of the pertinent unified dual subproblem. As feasible regions of \mathcal{Q}_i and \mathcal{O}_i remain the same in all iterations, $(\hat{\boldsymbol{\mu}}_i, \hat{\boldsymbol{\omega}}_i)$ is also a feasible solution for the unified dual subproblem when the tentative solution is $\bar{\mathbf{x}}'$. Given $(\hat{\boldsymbol{\mu}}_i, \hat{\boldsymbol{\omega}}_i)$ is the optimal solution of the unified dual subproblem, we have:

$$(\mathbf{e}'_i - \mathbf{B}'_i \bar{\mathbf{x}}')^T \hat{\boldsymbol{\mu}}_i + \mathbf{1}^T \hat{\boldsymbol{\omega}}_i \geq (\mathbf{e}'_i - \mathbf{B}'_i \bar{\mathbf{x}}')^T \boldsymbol{\mu}_i + \mathbf{1}^T \boldsymbol{\omega}_i, \quad \forall (\boldsymbol{\mu}_i, \boldsymbol{\omega}_i) \in \mathcal{Q}_i, \boldsymbol{\omega}_i \in \mathcal{O}_i$$

which further implies:

$$0 \geq (\mathbf{e}'_i - \mathbf{B}'_i \bar{\mathbf{x}}')^T \hat{\boldsymbol{\mu}}_i + \mathbf{1}^T \hat{\boldsymbol{\omega}}_i \geq (\mathbf{e}'_i - \mathbf{B}'_i \bar{\mathbf{x}}')^T \hat{\boldsymbol{\mu}}_i + \mathbf{1}^T \hat{\boldsymbol{\omega}}_i, \quad \forall (\hat{\boldsymbol{\mu}}_i, \hat{\boldsymbol{\omega}}_i)$$

Hence, any unified Benders cut in the following form does not eliminate $\bar{\mathbf{x}}'$: $(\mathbf{e}'_i - \mathbf{B}'_i \bar{\mathbf{x}}')^T \hat{\boldsymbol{\mu}}_i + \mathbf{1}^T \hat{\boldsymbol{\omega}}_i \leq 0, \quad \forall (\hat{\boldsymbol{\mu}}_i, \hat{\boldsymbol{\omega}}_i), \forall i$.

Similarly, let $(\hat{\mathbf{y}}_i, \hat{\mathbf{z}}_i)$ be the optimal solution for $(\mathbf{y}_i, \mathbf{z}_i)$ such that $(\hat{\mathbf{y}}_i, \hat{\mathbf{z}}_i)$ is also the optimal solution of the unified primal subproblem with the following constraint satisfied under $\bar{\mathbf{x}}'$ (when all slack variables are zero): $\mathbf{C}'_i \hat{\mathbf{y}}_i + \mathbf{D}'_i \hat{\mathbf{z}}_i \geq \mathbf{e}'_i - \mathbf{B}'_i \bar{\mathbf{x}}', \quad \forall i$

which means $(\hat{\mathbf{y}}_i, \hat{\mathbf{z}}_i)$ is not affected as long as $\bar{\mathbf{x}}'$ is not eliminated. In conclusion, the proposed unified Benders cuts do not eliminate the optimal solution of the original problem (4a)-(4d).

B. Complete Proposed Iterative Solution Process

Here we summarize the iterative solution steps based on modified Benders decomposition as follows:

Step 1: Initialize (by DSO). Formulate the initial master problem (9a)-(9b) without any additional cutting planes.

Step 2: Solve the master problem (by DSO). Solve (9a)-(9c) with newly-generated unified Benders cuts and feasibility restoration cuts (if any) and update the optimal solution $\bar{\mathbf{x}}'$ for interconnection network operations.

Step 3: Receive the master problem solution (in parallel by all MCs). If there is a new DSO solution $\bar{\mathbf{x}}'$, go to Step 4; otherwise, stay in Step 3.

Step 4: Solve the unified dual subproblem (in parallel by all MCs). Solve (13a) with $\bar{\mathbf{x}}'$ and update the optimal solution $(\hat{\boldsymbol{\mu}}_i, \hat{\boldsymbol{\omega}}_i)$ to form the unified Benders cut (13b). If $F_{D,i}^*$ achieves a positive value, go to Step 6; otherwise, go to Step 5.

Step 5: Solve the feasibility restoration subproblem (in parallel by all MCs). Solve (14a)-(14c) with $\bar{\mathbf{x}}'$ and update the optimal solution $(\hat{\mathbf{y}}_i, \hat{\mathbf{z}}_i)$. If $F_{F,i}^*$ achieves a positive value, generate the feasibility restoration cut (14i).

Step 6: Return cutting planes (in parallel by all MCs). If there exist newly-generated cutting planes, pass them to DSO; otherwise, go back to Step 3.

Step 7: Check convergence (by DSO). If there exists any new cutting plane provided by MCs, go back to Step 2; otherwise, terminate the iteration and output $\bar{\mathbf{x}}'$ and $(\hat{\mathbf{y}}_i, \hat{\mathbf{z}}_i)$ as the optimal operations for the interconnection network and microgrid i ($\forall i$), respectively.

C. Proof of Theorem 2

Theorem 2: The proposed iterative solution process based on modified Benders decomposition converges to the optimal solution of the original problem (4a)-(4d) in finite iterations.

Proof: First, we prove that the proposed solution process terminates in finite iterations. At each iteration, each MC evaluates the feasibility of the tentative master problem solution $\bar{\mathbf{x}}'$ and checks it against the unified Benders cut (13b). If it violates (13b), then (13b) alone reduces the feasible region of the original optimization problem by excluding $\bar{\mathbf{x}}'$ from interconnection network operations; otherwise, the feasibility restoration cut (14i) is generated to exclude $\bar{\mathbf{x}}'$ from the feasible region. Thus, the feasible region gradually shrinks as the iteration continues. Given that the feasible region is finite, the solution process would eventually be terminated.

Next, we prove that not all generated cutting planes exclude the optimal solution of the original problem (4a)-(4d). We have already proved in Theorem 1 that unified Benders cuts do not eliminate the optimal solution. Similarly, we prove feasibility restoration cuts do not eliminate the optimal solution. Again, let $\bar{\mathbf{x}}'$ be the optimal solution for \mathbf{x}' in the original optimization problem such that $\bar{\mathbf{x}}'$ is always a feasible solution of the feasibility restoration subproblem (14a)-(14c). Then for any infeasible $\hat{\mathbf{x}}'$, we have $\Delta_i(\bar{\mathbf{x}}', \hat{\mathbf{x}}') \geq \min_{\mathbf{x}'} \Delta_i(\mathbf{x}', \hat{\mathbf{x}}') = F_{F,i}^*, \quad \forall i$.

Accordingly, any feasibility restoration cut in the following form does not eliminate $\bar{\mathbf{x}}'$: $\Delta_i(\mathbf{x}', \hat{\mathbf{x}}') \geq F_{F,i}^*, \quad \forall i$. Let $(\hat{\mathbf{y}}_i, \hat{\mathbf{z}}_i)$ be the optimal solution for $(\mathbf{y}_i, \mathbf{z}_i)$. We conclude $(\hat{\mathbf{y}}_i, \hat{\mathbf{z}}_i)$ is not affected as long as $\bar{\mathbf{x}}'$ is not eliminated. Hence, feasibility restoration cuts do not eliminate the optimal solution of the original problem.

Last, we prove that the optimal solution to the original problem can be reached by the proposed iterative solution method. Since the optimal solution to the original problem satisfies master problem constraints, the master problem is a relaxation of the original problem in finding the optimal solution for \mathbf{x}' . Let $\bar{\mathbf{x}}'$ be the optimal solution of the master problem when the iterative process is terminated. Here, $\bar{\mathbf{x}}'$ is also a feasible solution for \mathbf{x}' in the original problem because $\bar{\mathbf{x}}'$

satisfies all master problem constraints and corresponds with no feasibility violations in feasibility restoration subproblems. In fact, \bar{x} ' is the optimal solution for the relaxed version of the original problem (i.e., master problem) so that \bar{x} ' is the optimal solution for x ' in the original problem. Given \bar{x} ', the optimal solution for each set of (y_i, z_i) is easily found by solving the feasibility restoration subproblem. In conclusion, this theorem is proved.

D. Test System Configuration and Results

1) Test System Configuration

Base values of power and voltage magnitude are set at 1 MVA and 4.16 kV. Bus 1 interfaces with the utility grid which has a fixed voltage magnitude of 1.0 p.u., while other bus voltage magnitudes are limited to be between 0.9 p.u. and 1.1 p.u. Buses 83, 88, 113, and 117 are equipped with SVCs, while six microgrids are connected to the distribution feeder via Buses 7, 50, 58, 96, 104 and 121. We consider six time intervals for operation, when conventional DGs are assumed to be initially OFF. The load curtailment costs are unified at 500 \$/MWh at all buses throughout the operation horizon. Fig. A.1 shows the topology of the modified IEEE 123-bus test system. Table A.I lists the detailed configurations of SVCs. Tables A.II, A.III and A.IV list characteristics of conventional DGs, renewables-based DGs, and ESSs in the six microgrids, respectively. Bus loads and power outputs of renewable DGs vary uniformly with time. The utility energy price, bus load, and renewable DG power forecasts are obtained by multiplying scalars in Table A.V with corresponding nominal values.

2) Numerical Experiment Results

Fig. A.2 shows the iterative communications between DSO and MCs for realizing their leader-follower partnership. Table A.VI lists the detailed power outputs of energy generation resources in all microgrids over the entire operation horizon. Fig. A.3 shows the relaxation errors of converged branch flow solutions for using the modified Benders decomposition. Fig. A.4 shows the convergence of bus voltage magnitudes in the local utility grid which satisfies the voltage security requirements. Figs. A.5 and A.6 show real and reactive power exchanges between microgrids and the local utility grid, respectively.

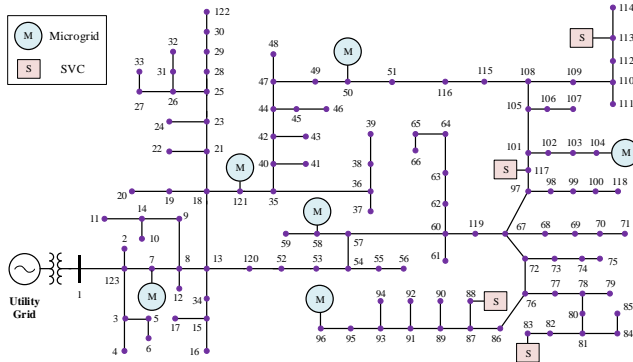


Fig. A.1 Modified IEEE 123-bus test system

TABLE A.I
SVC PARAMETERS

Bus	Output Range (kVar)	Bus	Output Range (kVar)
3	[-300, 300]	113	[-200, 200]
88	[-300, 300]	117	[-400, 400]

TABLE A.II
PARAMETERS OF CONVENTIONAL DGs

Bus	Production Cost (\$/kWh)	Start-Up Cost (\$)	Power Output Range		Ramping (kW)
			Real (kW)	Reactive (kVar)	
7	0.05	10	[20, 100]	[-50, 50]	50
50	0.08	5	[30, 150]	[-75, 75]	45
58	0.04	10	[50, 150]	[-50, 100]	80
96	0.055	10	[20, 120]	[-10, 50]	50
104	0.085	10	[10, 80]	[-20, 50]	40
121	0.045	10	[20, 120]	[-25, 75]	50

TABLE A.III
RENEWABLES DG PARAMETERS

Bus	Forecast Output (kW)	Min Power Factor	Bus	Forecast Output (kW)	Min Power Factor
50	50	0.95	104	40	0.85
58	80	0.85	121	60	0.9

TABLE A.IV
ESS PARAMETERS

Bus	Max Dis/charging Power (kW)	Energy Level (kWh)			Dis/charging Efficiency
		Min	Max	Initial	
7	40/40	20	80	60	0.9/0.9
50	40/40	20	100	40	0.85/0.85
58	35/35	30	90	30	0.9/0.9
96	60/60	40	160	80	0.95/0.95
104	40/40	20	80	40	0.9/0.9
121	30/30	40	120	60	0.9/0.9

TABLE A.V
SCALARS OF OPERATING CONDITIONS

Element	t=1	t=2	t=3	t=4	t=5	t=6
Price	0.77	1	1.16	0.9	1.30	0.77
Load	0.85	0.95	0.9	1	0.95	0.85
Renewables	1	1.2	0.6	1	1.4	1

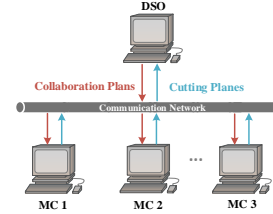


Fig. A.2 Data exchanges between DSO and MCs

TABLE A.VI
POWER OUTPUTS OF MICROGRID RESOURCES

Microgrid		Power Output (kW+jkVar)					
		t=1	t=2	t=3	t=4	t=5	t=6
1	DG	50+j50	100+j50	100+j50	100+j50	100+j50	50+j50
	RE	30+j14.5	36+j17.4	18+j8.7	30+j14.5	42+j20.3	30+j14.5
	ESS	-22.2	0	40	-32.1	40	0
2	DG	45+j75	90+j75	135+j75	150+j75	150+j75	150+j75
	RE	50+j16.4	60+j19.7	30+j9.9	50+j16.4	70+j23	50+j16.4
	ESS	-40	0	5.9	0	40	0
3	DG	80+j100	150+j100	150+j100	150+j100	150+j100	150+j100
	RE	80+j49.6	96+j59.5	48+j29.7	80+j49.6	112+j69.4	80+j49.6
	ESS	-35	0	21.7	-35	35	0
4	DG	50+j50	100+j50	120+j50	120+j50	120+j50	120+j50
	RE	80+j38.7	96+j46.5	48+j23.2	80+j38.7	112+j54.2	80+j38.7
	ESS	-60	0	60	-30.9	60	0
5	DG	0	0	0	0	0	0
	RE	40+j24.8	48+j29.7	24+j14.9	40+j24.8	56+j34.7	40+j24.8
	ESS	-40	0	40	-36.5	40	0
6	DG	50+j75	100+j75	120+j75	120+j75	120+j75	120+j75
	RE	60+j29.1	72+j34.9	36+j17.4	60+j29.1	84+j40.7	60+j29.1
	ESS	-30	0	30	-21.9	30	0

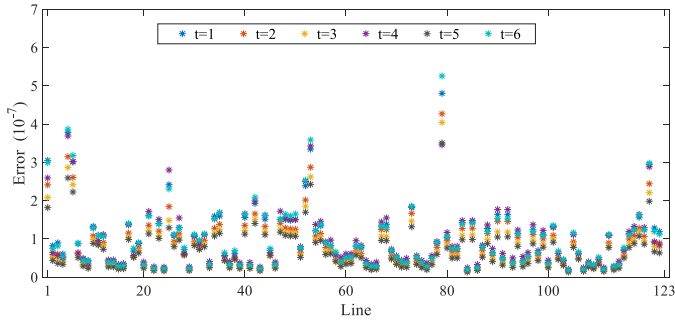


Fig. A.3 Second-order cone relaxation error

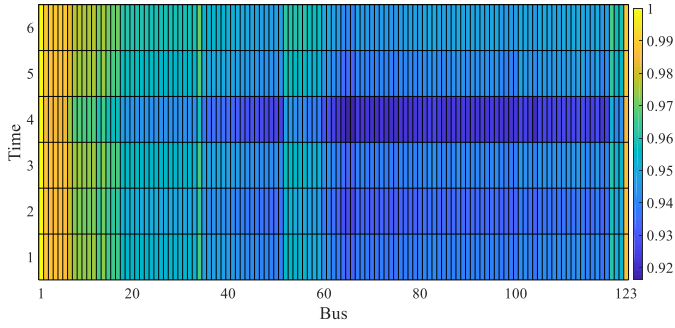


Fig. A.4 Voltage magnitude variations (p.u.)

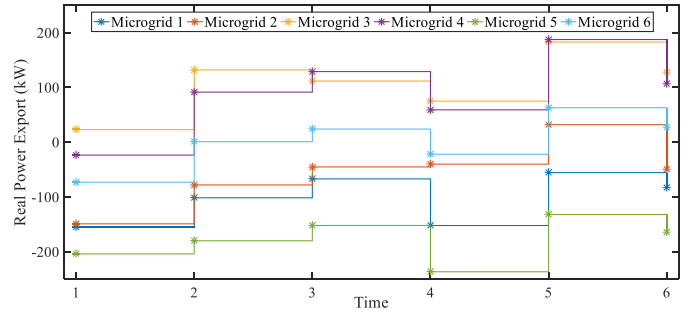


Fig. A.5 Optimal real power export of individual microgrids

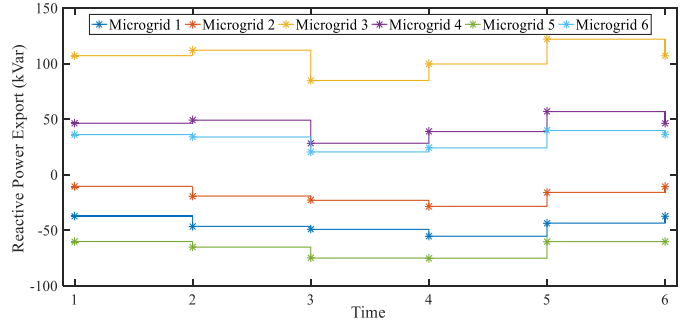


Fig. A.6 Optimal reactive power export of individual microgrids